05

Amplitude noise of 89X nm-range single-mode intracavity-contacted vertical-cavity surface-emitting lasers

© S.A. Blokhin[1], M.A. Bobrov[1], Ya.N. Kovach[1], A.A. Blokhin[1], M.N. Marchiy[1], N.A. Kuzmenkov[1], A.S. Pazgalev[1], A.G. Kuzmenkova[1], A.P. Vasyl'ev[2], N.A. Maleev[1]

[1] Ioffe Institute,
St. Petersburg, Russia
[2] Submicron Heterostructures for Microelectronics, Research & Engineering Center, RAS,
St. Petersburg, Russia

e-mail: blokh@mail.ioffe.ru

Received June 09, 2025
Revised June 09, 2025
Accepted August 14, 2025

In this work, we study the spectral density of the relative intensity noise (amplitude noise) of the 89X nm range single-mode vertical-cavity surface-emitting lasers with hybrid microcavity and carrier injection through the intracavity contacts and composite Bragg reflector. Carried analysis of the laser amplitude noise behavior demonstrated $1/f$-noise dependance for low frequencies with the transition to white noise at 10 kHz and higher. The amplitude noise dependance from the laser optical power showed *W*-like shape behavior. An increase in temperature led to an increase in amplitude noise both at a fixed operating current and at a comparable laser optical power. It was shown that developed lasers have amplitude noise lower than $1-100$ kHz in the frequency range -120 dB/Hz (depending on temperature and optical power) which allows to use them in compact atomic sensors of various types.

Keywords: vertical-cavity surface-emitting laser, relative intensity noise, amplitude noise, quantum sensors.

DOI: 10.61011/EOS.2025.08.62022.8251-25

In recent years, significant attention has been given to the development of compact quantum sensors based on vapors of alkali metal atoms (^{133}Cs, ^{85}Rb or ^{87}Rb), where laser emitters are used for optical pumping and/or detection [1,2]. The most promising direction is the use of vertical-cavity surface-emitting lasers (VCSELs) [3]. Laser emitters for compact atomic sensors must meet a specific set of requirements: single-mode operation, the ability for precise wavelength tuning to the alkali atom absorption line, narrow spectral linewidth, stable linear polarization of the emission, high speed at low operating currents, the ability to operate at elevated temperatures (depending on the design of the gas cell and quantum sensor configuration), low power consumption, and low noise levels. Most of the proposed designs for creating single-mode polarization-stable VCSELs in the spectral ranges 75X/79X nm and 85X/89X nm are based on the use of a vertical microcavity with carrier injection through doped distributed Bragg reflectors (DBRs) [4–8]. However, the published works predominantly focus on stabilizing the polarization state of emission, ensuring the required optical power level in single-mode operation, and/or laser speed at a given temperature, while issues related to minimizing relative intensity noise (RIN) or amplitude noise of the laser in the low-frequency range have received little attention. Meanwhile, the signal-to-noise ratio for quantum sensors is determined not only by the inherent noise of the photodetector but also by the amplitude noise of the laser, which ideally should be minimized to the photodetector shot noise level at detection frequencies (below -120 dB/Hz) [4].

It is known that the spectral density of noises in an injection laser at low frequencies typically exhibits two regions: a flicker-noise region caused by fluctuations in charge carrier mobility and density in semiconductor regions, and a white noise region caused by quantum fluctuations of spontaneous emission [9,10]. However, mode-beating processes and the presence of sub-threshold modes emitting in spontaneous regimes can cause excess low-frequency noise or its sharp increase with pump current [11,12]. Moreover, there is a correlation between low-frequency RIN and fluctuations of the injection current (so-called electrical noise) [9,13]. Consequently, alongside the classical flicker noise of $1/f$-type, generation-recombination processes via traps, known as generation-recombination noise with an $1/f^2$-type dependence, can significantly influence the fluctuations in charge carrier density in the active region [14]. Unlike edge-emitting lasers, VCSELs are characterized by a large number of internal heterointerfaces and potential barriers (primarily in thick doped DBRs), which can result in a more complex frequency dependence of electrical noise in the pump current, as seen, for example, in multimode VCSELs with an 850 nm spectral range and proton-implanted current apertures [15]. Furthermore, it was shown in [16] that the spectral density of current noise in a multimode 850 nm VCSEL with a selectively oxidized current aperture grows nonlinearly with pump current: at low currents,

there is a linear dependence of electrical noise on current, while at higher currents, the dependence becomes quadratic. However, injection lasers based on AlGaAs/GaAs material systems suffer from generation-recombination noise, leading to a more abrupt increase in electrical noise with pump current [13]. As a result, for VCSELs with conventional microcavity designs, the RIN noise in the low-frequency range is expected to depend not only on frequency but also on pump current (optical power).

Relatively recently, we proposed an alternative VCSEL design in the 85X/89X nm spectral range based on a hybrid vertical microcavity with carrier injection through intracavity contact layers and composite Bragg gratings (hereafter referred to as the hybrid microcavity concept) [17–19]. This design not only reduces internal optical losses and narrows the spectral linewidth but may also help suppress the adverse effects of charge carrier transport on electrical noise. This work presents research results on the spectral density of amplitude noise in single-mode polarization-stable VCSELs in the 89X nm spectral range, implemented within the hybrid microcavity concept.

The object of study is a semiconductor injection laser based on a hybrid vertical microcavity with upward vertical emission, structurally consisting of an undoped GaAs substrate, a bottom distributed Bragg reflector (DBR) based on quarter-wavelength layers $Al_{0.15}Ga_{0.85}As/Al_{0.9}Ga_{0.1}As$, a bottom intracavity contact layer of $Al_{0.15}Ga_{0.85}As$ *n*-type, a bottom composite Bragg grating of *n*-type based on layers *n*-$Al_{0.15}Ga_{0.85}As$/*n*-$Al_{0.9}Ga_{0.1}As$ with graded interfaces at heterojunctions, an optical resonant cavity of $Al_{0.15}Ga_{0.85}As$ with active region, a top composite Bragg grating of $Al_{0.15}Ga_{0.85}As/Al_{0.9}Ga_{0.1}As$ *p*-type with a selectively oxidized aperture, a top intracavity contact layer of $Al_{0.15}Ga_{0.85}As$ *p*-type, and a top dielectric DBR based on quarter-wavelength layers SiO_2/Ta_2O_5. The active region comprises five 8 nm thick $In_{0.06}Ga_{0.94}As$ quantum wells, confined by $Al_{0.15}Ga_{0.85}As$ barriers. The current aperture is formed by selective oxidation in water vapor of a composite aperture layer $AlAs/Al_{0.9}Ga_{0.1}As$. Details of the heterostructure and device design of the 89X nm VCSEL are given in [18,19].

Figure 1, *a* shows the influence of ambient temperature on the current-voltage and power-current characteristics of the 89X nm VCSEL with a selectively oxidized current aperture size of 2 μm. At 20 °C the devices demonstrate laser generation with a differential efficiency of 0.57 A/W and a threshold current of 0.3 mA. The laser self-heating effect limits the maximum laser current. Since reaching the saturation point of output optical power is associated with strong overheating of the active region and rapid acceleration of laser degradation, the working current range was limited from above by a 50 % drop in differential efficiency. As the temperature increases to 80 °C not only does the saturation maximum working current decrease from 3.6 to $\sim$ 3 mA but the differential efficiency lowers to 0.47 A/W and the threshold current grows to 0.56 mA. The first behavior is primarily due to the growth of thermal resistance of the laser caused by worsening thermal conductivity of semiconductor materials. The second effect may be related both to suboptimal spectral detuning of the resonant wavelength relative to the gain profile of the active region and to decreased current injection efficiency with temperature increase. An analysis of these causes requires further study and is beyond the scope of this work.

An analysis of the spectral and polarization characteristics of the 89X nm VCSEL showed that laser generation occurs through the fundamental mode (so-called single-mode regime) across the entire investigated range of currents and temperatures (see inset in Fig. 1, *a*). Due to the diamond shape of the selectively oxidized current aperture, degeneracy of the fundamental mode is lifted, and the polarization of laser emission is fixed along the crystallographic direction $[\bar{1}10]$ with an orthogonal polarization suppression ratio (OPSR) above 20 dB [19]. With increasing temperature up to 80 °C a slight decrease in OPSR level is observed, apparently caused by a reduction in the ratio of stimulated emission to spontaneous emission.

Studies of the relative intensity noise (RIN) of laser emission were conducted using a digital synchronous amplifier (DSA) operating in noise density measurement mode within a 1 Hz bandwidth at a specified detuning from the carrier frequency. To improve the signal-to-noise ratio and ensure effective coupling of the low-noise photodetector (LNP) with the DSA amplifier, a current-to-voltage converter (CVC) was employed. To appropriately account for the frequency dependence of the CVC gain and losses in the electrical path connecting the output of the LNP photodetector and the input of the DSA amplifier, the corresponding transfer function G was determined. The root-mean-square total noise signal RMS_{total} was calculated based on registered in-phase and quadrature noise components with temporal averaging. The RIN noise level was determined by subtracting the thermal noise RMS_{th} of the registration system (measured in the absence of optical signal) from the total registered amplitude noise RMS_{total} followed by normalization to the transfer function G and the average photocurrent I_o (at the optical power P_o) incident on the photodetector): $RIN_{laser} = 20\log(\sqrt{RMS^2_{total} - RMS^2_{th}}/I_oG)$. A low-noise power supply combined with a low-pass filter with a cutoff frequency of 1.5 Hz was used to minimize the contribution of technical noise from the power supply. Due to the input current limitation of the CVC at laser output optical power above 0.6 mW, neutral density filters were used to attenuate the optical power measured by the photodetector.

Figure 2, *a* shows typical results of the spectral density study of relative intensity noise for single-mode VCSELs in the 89X nm spectral range, with a selectively oxidized current aperture size of 2 μm at 20 °C. To minimize noise when using pin-type connectors, the measurements were performed directly on the chips without packaging. It should be noted that technical noise of the measurement setup becomes noticeable only below 100 Hz, but it is two orders

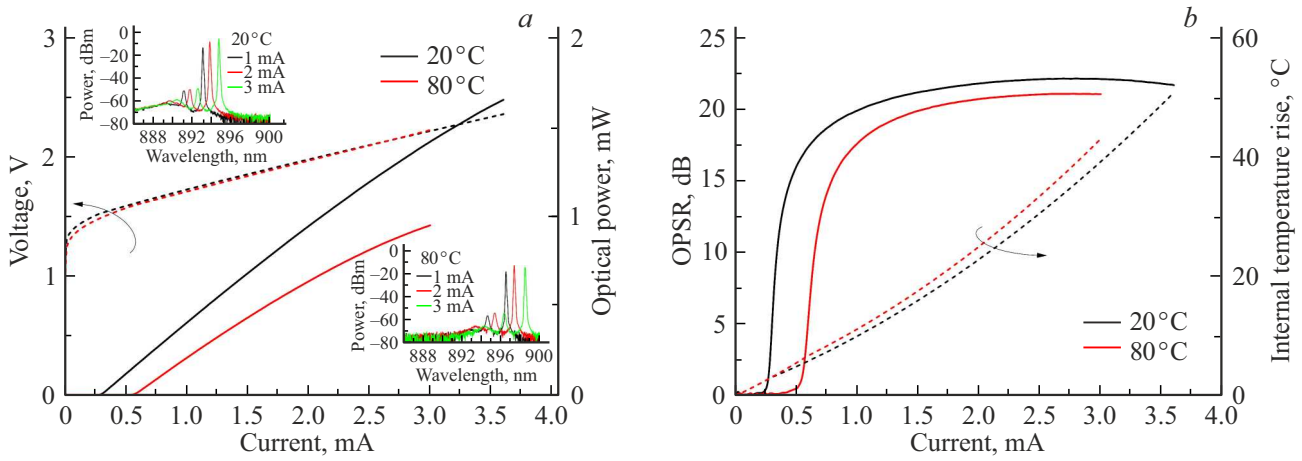

Figure 1. Static characteristics of 89X nm VCSELs with a characteristic selectively oxidized current aperture size of 2 μm at various temperatures: *a* — current-voltage and power-current characteristics. Insets show emission spectra at different currents. *b* — dependence of the orthogonally polarized mode suppression ratio (OPSR) on current.

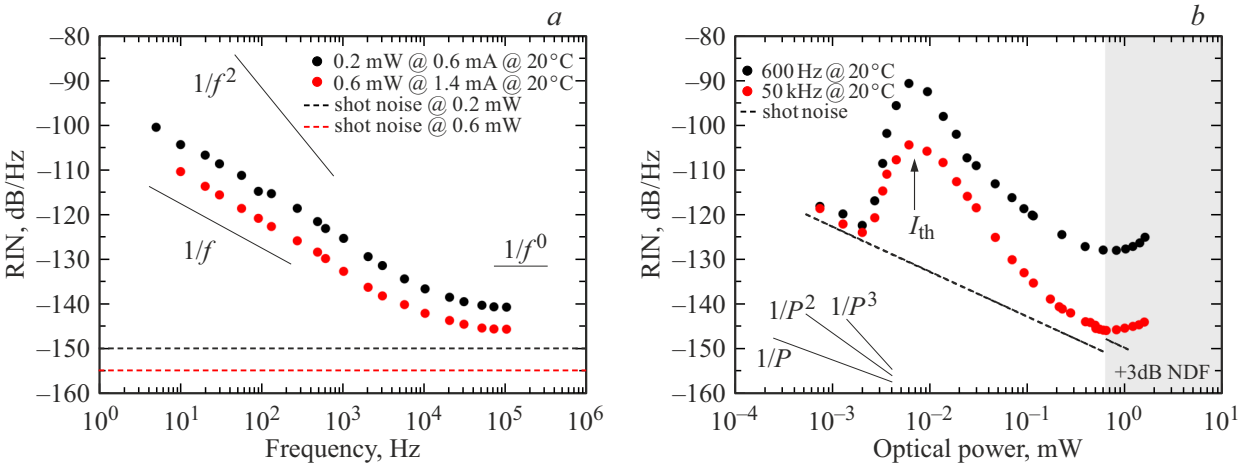

Figure 2. Spectral density of relative intensity noise (RIN) of emission for the hybrid VCSEL in the 89X nm spectral range with a selectively oxidized current aperture size of 2 μm at measurement temperature 20°C. *a* frequency dependence of RIN noise at different optical power levels. *b* dependence of RIN noise on incident optical power at different detection frequencies. The region of neutral density filter (NDF) usage with 3 dB attenuation is shaded in gray.

of magnitude lower than the registered laser noise levels and does not significantly affect the results. The RIN noise spectrum of the laser in the low-frequency region follows the characteristic $1/f^n$-type noise with a pronounced transition to white noise at frequencies above 10 kHz, where the noise level noticeably exceeds the photodetector shot noise level. Tripling the output optical power of the VCSEL leads not only to the expected reduction in white noise level [20] but also to that of the $1/f^n$-type noise, despite the rise in electrical noise. A slight shift of the transition boundary to white noise (hence transition $1/f$-$1/f^0$) towards lower frequencies is observed. The RIN noise decay rate with frequency (in the low-frequency region) depends weakly on optical power and is approximately $\sim$ 11 dB/Hz per decade, i.e., the dependence follows the classical $1/f$-type flicker noise, which correlates well with experimental data for single-mode polarization-stable VCSELs in the 79X nm [7], 85X nm [4] and 89X nm [6,21] spectral ranges based on the classical vertical microresonator design with carrier injection through doped DBRs.

Figure 2, *b* presents typical dependencies of RIN noise level of the studied lasers on incident optical power for various detection frequencies at 20 °C. It is evident that the characteristic behavior of RIN noise versus output optical power (pump current) depends on the detection frequency. In the spontaneous emission regime, an increase in output power (correlating with the laser generation threshold) leads to a sharp rise in RIN level [22] regardless of detection frequency, which can be explained by increased fluctuations in material gain [9]. Upon entering the stimulated emission regime, the behavior changes. At frequencies above 10 kHz, there is initially a pronounced drop in the laser RIN noise

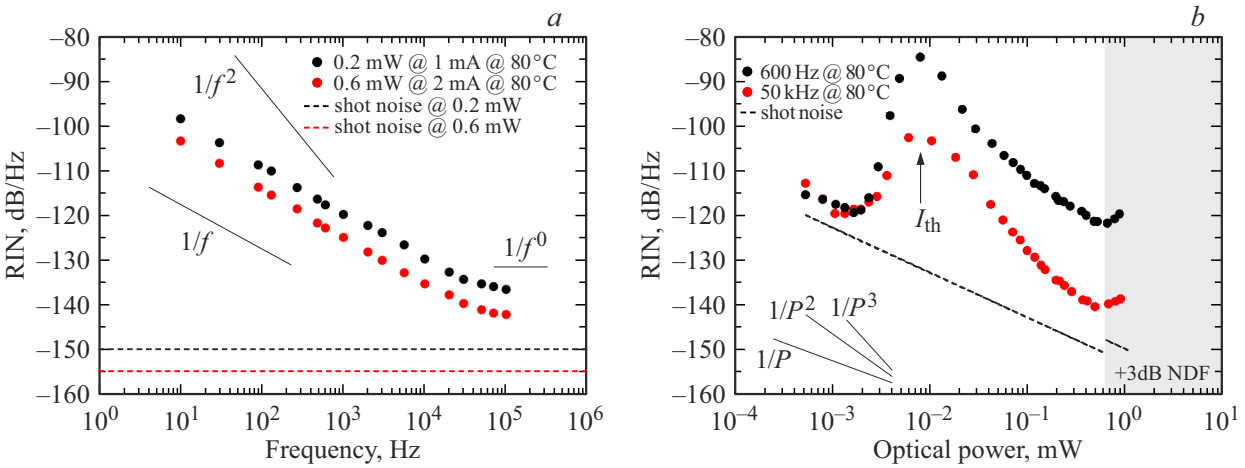

Figure 3. Spectral density of relative intensity noise (RIN) for the hybrid VCSEL in the 89X nm spectral range with selectively oxidized current aperture size of $2\,\mu$m at measurement temperature 80°C. *a* frequency dependence of RIN noise at various optical power levels. *b* dependence of RIN noise on incident optical power at different detection frequencies. The region of neutral density filter (NDF) usage with 3 dB attenuation is shaded in gray.

followed by rapid saturation at a level of 145 dB/Hz, still exceeding the photodetector shot noise level, and then an increase in noise level with incident optical power above 1 mW (i.e., realization of an *W*-type dependence). The white noise decay rate is$\sim$ 30 dB/Hz per decade, consistent with results for VCSELs in the near-infrared range [23,24]. At frequencies below 1 kHz, a sharp decrease in noise decay rate with increasing optical power to $\sim$ 15 dB/Hz per decade is observed, with RIN saturation occurring at somewhat lower incident optical power values and a more well-defined *W*-type dependence. Thus, as the output optical power in the lasing regime increases, an initial decrease in RIN noise is observed, correlating with results for single-mode polarization-stable VCSELs in the 89X nm spectral range [21], but at powers above 0.6 mW, a reverse trend of RIN noise increase in the low-frequency region occurs. Overall, the obtained RIN noise values in the white noise region are significantly lower than those reported for classical VCSELs in the 76X nm [25] and 79X nm [7] spectral ranges and correlate well with data for 85X nm [4] and 89X nm [6].

Anomalous RIN noise dependence at comparable optical power was also observed for single-mode VCSELs in the 76X nm spectral range with an air current aperture [25], but there the RIN noise increase was found in the high-frequency range where white noise typically appears and was attributed to polarization instability. However, analysis of the modal composition and polarization state of the studied lasers revealed no evidence of transverse mode beating or polarization switching, despite lifting the degeneracy of the fundamental polarization mode.

Similar RIN noise behavior was previously reported for multimode VCSELs at 850 nm spectral range with proton-implanted current apertures [13,15], explained by peculiarities of charge carrier transport in that specific VCSEL design. Moreover, generation-recombination noise in AlGaAs/GaAs-based injection lasers can lead to a shift of the transition boundary from an $1/f$ type to an $1/f^0$ type dependence and a marked exceeding of the shot noise level [13]. However, in our case, the opposite trend is observed for the transition boundary $1/f$-$1/f^0$.

Taking into account the high thermal resistance of the studied VCSELs ($\sim$ 7 K/mW), it was hypothesized that this behavior is related to thermal effects due to laser self-heating. To verify this, temperature-dependent studies of RIN noise were conducted. It is evident that at a fixed pump current, increasing temperature leads to a rise in RIN noise, which can be associated with decreased laser output optical power. However, even at comparable incident power values (adjusted by changing operating current), an increase in RIN noise with temperature and a shift of the $1/f$–to-white noise transition region towards higher frequencies is observed (Fig. 3, *a*). The character of the RIN spectral density behavior does not change, but an additive noise increase of $5-6$ dB, is observed, which can be interpreted as preservation of the mechanisms determining the frequency dependence of RIN noise. According to Fig. 3, *b*, no significant changes in the dependence of RIN noise on optical power were found apart from an additive noise increase, even in the white noise region.

Figure 1, *b* shows results of estimating the overheating of the laser active region, obtained based on analysis of shifts in the resonant wavelength with temperature and emitted power. The high thermal resistance of the VCSEL leads to rapid self-heating of the active region, surpassing 30 °C. at operating currents above 2.5 mA. However, increased active region temperature results in increased RIN noise, which causes saturation and growth of RIN noise at higher optical power (pump current) levels. The increase in ambient

temperature only intensifies the negative effect due to the rise in the laser's thermal resistance.

A somewhat similar influence of temperature on RIN noise was observed for single-mode VCSELs in the 76X nm spectral range with air current apertures [25] and was explained by the lasers' reduced efficiency at elevated temperatures, likely due to suboptimal spectral detuning between the resonant wavelength and the gain spectrum of the active region. However, temperature rise also enhances thermal carrier escape from the active region (reducing current injection efficiency), which, combined with suboptimal spectral detuning, leads not only to a significant increase in threshold current but also in the operating current at a given optical power (considering the drop in differential efficiency), and consequently to increased electrical noise. Identifying the causes of this additive noise increase requires further comprehensive investigations beyond the scope of the present work.

Thus, studies were carried out on the spectral density of relative intensity noise in single-mode VCSELs in the 89X nm spectral range with carrier injection through intracavity contact layers and composite Bragg gratings. The behavior of RIN noise and polarization noise of the lasers exhibits $1/f$–type noise with a well-defined transition to white noise. Increasing the optical emission power leads to a decrease in amplitude noise, saturating at the level of -145 dB/Hz in the frequency range $10-100$ kHz. Temperature increase results in an escalation of RIN noise both at fixed operating current and optical power. Nevertheless, at optical powers above 0.2 mW, the amplitude noise level in the $1-100$ kHz frequency range remains below -120 dB/Hz. The obtained results generally correlate with data for VCSELs in the 79X nm [7] and 85X nm [4] spectral ranges, as well as with data for 89X nm VCSELs [6,21] demonstrating polarization anisotropy and spatially selective losses, successfully tested in quantum frequency standards and/or quantum magnetometers. These research results are important for the development of laser emitters for quantum atomic sensors based on ^{133}Cs atoms.

Funding

This research was conducted with partial support from the Ministry of Science and Higher Education of the Russian Federation (project FFUG-2025-0006).

Conflict of interest

The authors declare that they have no conflict of interest.

References

[1] J. Kitching. Appl. Phys. Rev., **5** (3), 031302 (2018). DOI: 10.1063/1.5026238
[2] P. Zhou, W. Quan, K. Wei, Z. Liang, J. Hu, L. Liu, G. Hu, A. Wang, M.Ye. Biosensors, **12** (12), 1098 (2022). DOI: 10.3390/bios12121098
[3] B.D. Padullaparthi, J. Tatum, I. Kenichi. *VCSEL Industry: Communication and Sensing* (John Wiley & Sons, 2021).
[4] D.K. Serkland, K.M. Geib, G.M. Peake, R. Lutwak, A. Rashed, M. Varghese, G. Tepolt, M. Prouty In: *Vertical-Cavity Surface-Emitting Lasers XI*, ed. by K.D. Choquette, J.K. Guenter. Integrated Optoelectronic Devices (2007), p. 648406. DOI: 10.1117/12.715077
[5] J.D. Francesco, F. Gruet, C. Schori, C. Affolderbach, R. Matthey, G. Mileti, Y. Salvadé, Y. Petremand, N. De Rooij In: *Semiconductor Lasers and Laser Dynamics IV*, ed. by. K. Panajotov. SPIE Photonics Europe (2010), p. 77201T. DOI: 10.1117/12.854147
[6] F. Gruet, A. Al-Samaneh, E. Kroemer, L. Bimboes, D. Miletic, C. Affolderbach, D. Wahl, R. Boudot, G. Mileti, R. Michalzik. Opt. Express., **21** (5), 5781 (2013). DOI: 10.1364/OE.21.005781
[7] V.A. Gaisler, I.A. Derebezov, A.V. Gaisler, D.V. Dmitriev, A.K. Bakarov, A.I. Toropov, M.M. Kachanova, Y.A. Zhivodkov, A.V. Latyshev, M.N. Skvortsov, S.M. Ignatovich, V.I. Vishnyakov, N.L. Kvashnin, I.S. Mesenzova, A.V. Taichenachev, S.N. Bagaev, I.Y. Blinov, D.A. Parekhin, Optoelectron. Instrum. Data Process., **57** (5), 445–450 (2021). DOI: 10.3103/S875669902105006X
[8] Q. Fu, Y. Sun, S. Yu, A. Wang, J. Yin, Y. Zhao, J. Dong. Nanomaterials, **13** (6), 1120 (2023). DOI: 10.3390/nano13061120
[9] Y.L. Bessonov, N.B. Kornilova, V.D. Kurnosov, N.V. Moroz, S.D. Narolenko, C.M. Thai, V.R. Shidlovskii. Sov. J. Quantum Electron., **15** (11), 1567–1569 (1985). DOI: 10.1070/QE1985v015n11ABEH007990
[10] T. Suhara. *Semiconductor Laser Fundamentals* (CRC Press, 2004). DOI: 10.1201/9780203020470
[11] A.P. Bogatov, A.E. Drakin, S.A. Plisyuk, A.A. Stratonnikov, M.S. Kobyakova, A.V. Zubanov, A.A. Marmalyuk, A.A. Padalitsa. Quantum Electron., **32** (9), 809–814 (2002). DOI: 10.1070/QE2002v032n09ABEH002296
[12] A.P. Bogatov, P.G. Eliseev, O.A. Kobildzhanov, V.R. Madgazin, O.G. Okhotnikov, G.T. Pak, A.V. Khaĭdarov. Sov. J. Quantum Electron., **16** (12), 1596–1602 (1986). DOI: 10.1070/QE1986v016n12ABEH008476
[13] S.-L. Jang, J.-Y. Wu. Solid. State. Electron., **36** (2), 189–196 (1993). DOI: 10.1016/0038-1101(93)90138-G
[14] F.N. Hooge, T.G.M. Kleinpenning, L.K.J. Vandamme. Reports Prog. Phys., **44** (5), 479–532 (1981). DOI: 10.1088/0034-4885/44/5/001
[15] P. Signoret, G. Belleville, B. Orsal. Fluct. Noise Lett., **01** (01), L1–L5 (2001). DOI: 10.1142/S0219477501000044
[16] J. Zhang, W. Liao, X. Wang, G. Lu, S. Yang, Z. Wei. Photonics, **9** (11), 801 (2022). DOI: 10.3390/photonics9110801
[17] M.A. Bobrov, N.A. Maleev, S.A. Blokhin, A.G. Kuzmenkov, A.P. Vasil'ev, A.A. Blokhin, Y.A. Guseva, M.M. Kulagina, Y.M. Zadiranov, S.I. Troshkov, V. Lysak, V.M. Ustinov. Semiconductors, **50** (10), 1390–1395 (2016). DOI: 10.1134/S1063782616100092
[18] S.A. Blokhin, N.A. Maleev, M.A. Bobrov, A.G. Kuz'menkov, A.P. Vasil'ev, Y.M. Zadiranov, M.M. Kulagina, A.A. Blokhin, Y.A. Guseva, A.M. Ospennikov, M.V. Petrenko, A.G. Gladyshev, A.Y. Egorov, I.I. Novikov, L.Y. Karachinsky, D.V. Denisov, V.M. Ustinov. Quantum Electron., **49** (2), 187–190 (2019). DOI: 10.1070/QEL16871
[19] S.A. Blokhin, Y.N. Kovach, M.A. Bobrov, A.A. Blokhin, N.A. Maleev. St. Petersbg. Polytech. Univ. J. Phys. Math., **16** (3), 16–22 (2023). DOI: 10.18721/JPM.163.202

[20] M. Yamada. IEEE J. Quantum Electron., **22** (7), 1052–1059 (1986). DOI: 10.1109/JQE.1986.1073087
[21] E. Kroemer, J. Rutkowski, V. Maurice, R. Vicarini, M.A. Hafiz, C. Gorecki, R. Boudot. Appl. Opt., **55** (31), 8839 (2016). DOI: 10.1364/AO.55.008839
[22] A.V. Marugin, A.V. Kharchev, V.B. Tsaregradsky. ZhTF, **64** (5), 62 (1994) (in Russian).
[23] F. Koyama, K. Morito, K. Iga. IEEE J. Quantum Electron., **27** (6), 1410–1416 (1991). DOI: 10.1109/3.89958
[24] D.M. Kuchta, J. Gamelin, J.D. Walker, J. Lin, K.Y. Lau, J.S. Smith, M. Hong, J.P. Mannaerts. Appl. Phys. Lett., **62** (11), 1194–1196 (1993). DOI: 10.1063/1.108731
[25] H.P. Zappe, F. Monti di Sopra, H.-P. Gauggel, K.H. Gulden, R. Hovel, M. Moser. In: *Laser Diodes and LEDs in Industrial, Measurement, Imaging, and Sensors Applications II; Testing, Packaging, and Reliability of Semiconductor Lasers V*, ed. by G.T. Burnham. Symposium on Integrated Optoelectronics (SPIE, 2000), p. 106. DOI: 10.1117/12.380526

Translated by J.Savelyeva